Quantum Oscillations and High Carrier Mobility in the Delafossite $PdCoO_2$

Clifford W. Hicks,[1] Alexandra S. Gibbs,[1,2] Andrew P. Mackenzie,[1,*] Hiroshi Takatsu,[3] Yoshiteru Maeno,[4] and Edward A. Yelland[1,5]

[1]*Scottish Universities Physics Alliance (SUPA), School of Physics and Astronomy, University of St. Andrews, St. Andrews KY16 9SS, United Kingdom*
[2]*School of Chemistry and EaStCHEM, University of St. Andrews, North Haugh, St. Andrews KY16 9ST, United Kingdom*
[3]*Department of Physics, Tokyo Metropolitan University, Tokyo 192-0397, Japan*
[4]*Department of Physics, Graduate School of Science, Kyoto University, Kyoto 606-8502, Japan*
[5]*SUPA, School of Physics and Astronomy, and Centre for Science at Extreme Conditions, University of Edinburgh, Mayfield Road, Edinburgh EH9 3JZ, United Kingdom*

(Received 20 February 2012; published 10 September 2012)

We present de Haas–van Alphen and resistivity data on single crystals of the delafossite $PdCoO_2$. At 295 K we measure an in-plane resistivity of 2.6 $\mu\Omega$ cm, making $PdCoO_2$ the most conductive oxide known. The low-temperature in-plane resistivity has an activated rather than the usual T^5 temperature dependence, suggesting a gapping of effective scattering that is consistent with phonon drag. Below 10 K, the transport mean free path is $\sim$20 μm, approximately 10^5 lattice spacings and an astoundingly high value for flux-grown crystals. We discuss the origin of these properties in light of our data.

DOI: 10.1103/PhysRevLett.109.116401 PACS numbers: 71.18.+y, 71.20.Be, 72.10.Di, 72.15.Eb

A number of discoveries, for example graphene and the superconductivity in the sodium cobaltate system, have focused attention on the properties of two-dimensional conduction on triangular lattices. One of the most prominent families of such materials is the delafossites ABO_2, where the A atoms (Pt, Pd, Ag or Cu) are directly bonded to each other in triangular-lattice sheets, separated by BO_2 layers. Possibilities for B include Cr, Co, Fe, Al and Ni [1,2]. The delafossite family includes band insulators and semiconductors [2,3], transparent semiconductors [4], metallic magnets [5], candidate thermoelectrics [6], and magnetic and magnetoelectric insulators [7]. There are also nonmagnetic metals that present a combination of strong anisotropy, high carrier density and high mobility that is unique for bulk materials [3,8]. Here, we concentrate on the most extensively studied material, $PdCoO_2$.

$PdCoO_2$ crystallizes in the space group $R\bar{3}m(D_{3d}^5)$. The lattice parameters of the hexagonal unit cell at 298 K are $a = b = 2.830$ Å, and $c = 17.743$ Å [9]. Single crystals have been grown by several groups [9–11]. The Co atoms have formal valence +3 and configuration $3d^6$, and calculations place the Fermi level E_F between filled pseudo-t_{2g} and empty pseudo-e_g levels [12–14]. The Pd sheets therefore dominate the conductivity, leading to high transport anisotropy. The Pd atoms have formal valence +1, in configuration $4d^{9-x}5s^x$. A key issue in understanding the physics of $PdCoO_2$ is the relative importance of the $4d$ and $5s$ states to the conduction. We will return to this in light of our data.

$PdCoO_2$ is nonmagnetic, and so shows none of the frustration effects commonly associated with magnetism in triangular lattices. Band structure calculations [12,15] and angle-resolved photoemission spectroscopy (ARPES) data [10] indicate that it has a broad, half-filled conduction band, leading to a single, nearly two-dimensional Fermi surface (FS) with a rounded hexagonal cross section. This is different from graphene or graphite, since the Pd atoms form a simple triangular array rather than a honeycomb lattice.

At room temperature, $PdCoO_2$ is the most conductive oxide known. To measure the in-plane resistivity ρ_{ab}, we cut three needlelike samples from a 6 μm-thick single crystal, of length $\sim$400 μm and widths 39, 42 and 120 μm. The measured resistances of all samples were consistent with $\rho_{ab}(295\ \mathrm{K}) = 2.6(2)\ \mu\Omega$ cm: two and four times, respectively, less resistive than other oxides known for their high conductivity, $SrMoO_3$ and ReO_3 [16,17]. Among the elemental metals, only Cu, Ag and Au have lower resistivities (1.7, 1.6 and 2.2 $\mu\Omega$ cm, respectively). The high conductivity of $PdCoO_2$ is especially surprising considering that the CoO_2 layers do not contribute itinerant carriers: the carrier density is 30% that of Cu.

To study the origin of this high conductivity, we combined a de Haas–van Alphen (dHvA) study, using a piezoresistive torque method [18], with high-resolution resistivity measurements. The crystals were grown as described in Ref. [9]. They are clean: the resistivity samples have $\rho_{ab}(295\ \mathrm{K})/\rho_{ab}(0) \approx 250$. Torque measurements were carried out between 50 mK and 20 K, on a crystal $\approx$120 μm across and 30 μm thick; example torque data are shown in Fig. 1. That the measurement current was not heating the samples was checked with simultaneous measurement of dHvA oscillations in Sr_2RuO_4, a renormalized Fermi liquid with well-known quasiparticle masses. Using a rotatable sample stage, the field $\mathbf{H}$ could be rotated by an

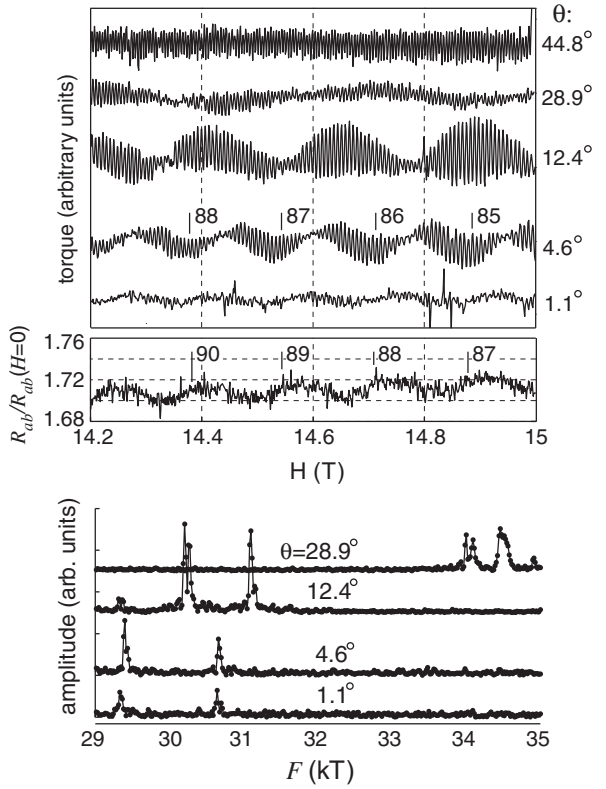

FIG. 1. Upper panel: torque curves against H, at the indicated angles θ between **H** and the c axis, and magnetoresistance of a resistivity sample. The ticks on this curve and the 4.6° torque curve label the cycle number of the difference frequency: the troughs in the resistance oscillations match up with points where the torque oscillation amplitude (and likely magnetic interaction) is largest. Lower panel: Fourier transforms over the field range 8.1–15 T.

angle θ from the crystal c axis toward the F symmetry point of the first Brillouin zone (as illustrated in Fig. 2). The temperature dependence of the dHvA effect was studied at $\theta = -6°$, and the θ dependence at $T = 0.7$ K.

The data in Fig. 1 are consistent with $PdCoO_2$ being a high purity, high carrier concentration, quasi-2D metal. At each angle θ we observe two large dHvA frequencies that differ by only ~3%, and that vary approximately as $1/\cos(\theta)$, confirming the overall cylindrical form of the FS. We also observe significant magnetic interaction (MI), an effect seen in the highest purity metals [19]. Most torque curves show a common characteristic of MI, a strong difference frequency amplitude, visible in Fig. 1 as an oscillation matching the beating of the two high frequencies. The difference frequency also appears in the magnetoresistance, ruling out torque interaction as its origin.

Considerable insight into the physics of $PdCoO_2$ can be obtained from detailed analysis of the dHvA data. Following [20,21], the corrugations on nearly cylindrical Fermi surfaces can be expanded into harmonic components with amplitudes $k_{\mu\nu}$,

$$k_F(\phi, k_z) = \sum_{\mu,\nu} k_{\mu\nu} \cos\mu\phi \begin{Bmatrix} \cos\nu d k_z \\ \sin\nu d k_z \end{Bmatrix}, \quad (1)$$

where k_z is the z component of the wave vector, $d = c/3$ the interlayer spacing, and ϕ the azimuthal angle. k_{00} is the average radius of the FS, and the remaining $k_{\mu\nu}$ are the amplitudes of harmonic components of the corrugation. The lower-order components relevant to $PdCoO_2$ are illustrated in Fig. 2, along with the amplitudes fitted from experimental data. (The fitted frequencies are calculated by numerical integration. The online Supplemental Material [22] contains further discussion.)

Numerical integration of the volume enclosed by the FS yields a carrier density of 1.005(1) per formula unit, based on room-temperature values for a and b. If a and b shrink by ~0.25% at low temperatures then the carrier density becomes almost exactly one: the FS of $PdCoO_2$ arises, to high precision, from a single half-filled band.

As mentioned above, a key issue for understanding $PdCoO_2$ is the relative importance of the Pd $4d$ and $5s$ orbitals in states near the Fermi level. The dHvA masses [$m^* \equiv (\hbar^2/2\pi)dA/dE$, where A is the FS cross-sectional area] provide the first piece of evidence that the $5s$ component is more important than has usually been assumed. Our data yield $m^* = 1.45(5)m_e$ and $1.53(3)m_e$ for the 29.3 and 30.7 kT orbits, respectively (at $\theta = -6°$; see the Supplemental Material [22]), corresponding to an electronic specific heat of approximately 1 $\mathrm{mJ/mol\,K^2}$, in fairly good agreement with a measured value of 1.28 $\mathrm{mJ/mol\,K^2}$ [9,22]. These masses would be very low for a d orbital-derived FS. For comparison, Pd metal (which has atomic spacing 2.75 Å, just 3% less than in $PdCoO_2$) has a mainly $5s$-derived electronlike Fermi pocket, compensated by a $4d$-derived open hole surface, and the dHvA masses of these surfaces are ~2.0 and $5–10m_e$, respectively [23,24]. The $PdCoO_2$ dHvA masses are much closer to that of the Pd $5s$ than the Pd $4d$ surface.

The form of the FS warping also emphasizes the role played by the $5s$ component. The dominant warping is k_{01}, suggesting interlayer transport by direct Pd-Pd overlap, which would rely on the extended $5s$ component to cross the 6 Å interlayer separation. Hopping via the Co atoms would allow transport through the more compact d orbitals, but connects interlayer next-nearest-neighbor Pd sites (through the path Pd-O-Co-O-Pd, illustrated in Fig. 5b of [15]), leading to a large k_{31}. Published calculations indeed show bumps on the FS with significant Co character that give a large k_{31} [12,15]. The dHvA data, however, show that k_{01} is far larger than k_{31}.

Hybridization between the Pd $4d_{z^2}$ and $5s$ orbitals has been discussed in [3,13,25]. Reports on electronic structure calculations have tended to mention the likelihood of a $5s$ component at E_F but emphasize the $4d$ contribution [12–15]. However in a calculation of $PdCoO_2$ without the CoO_2 spacer layers, i.e., bare Pd sheets, a $5s$ manifold that

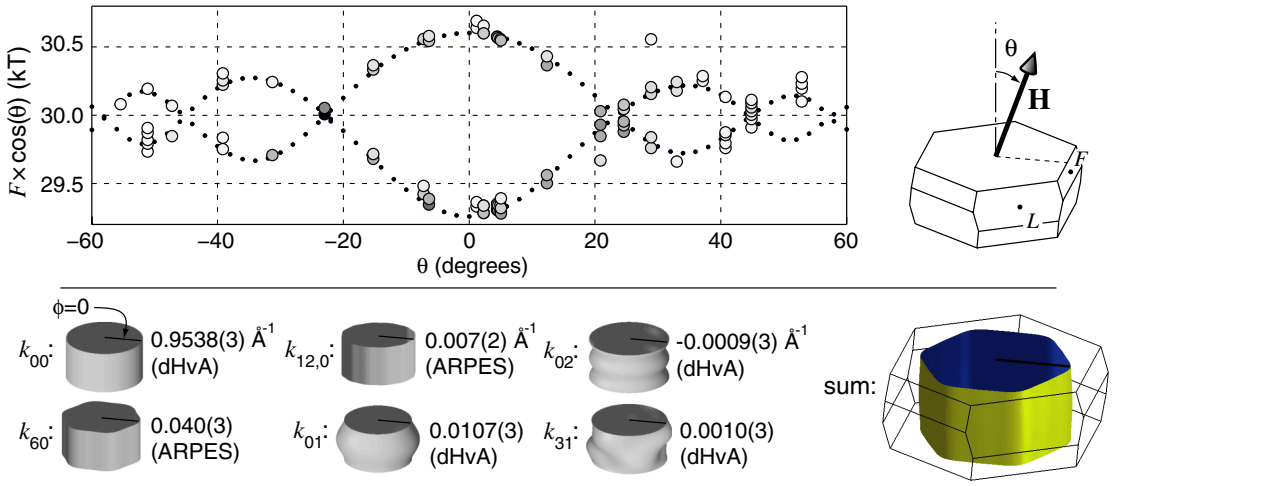

FIG. 2 (color online). Top: observed dHvA frequencies F, obtained by Fourier transform over the field range 8.1 to 15 T (circles; darker shading indicates larger amplitude), and a fit (small points). Bottom: the separate harmonic components included in the fit, and their amplitudes. k_{60} and $k_{12,0}$ are obtained from ARPES data [10], and k_{00}, k_{01}, $k_{02,}$ and k_{31} from the fit. k_{01} gives the overall Yamaji-type form to $F(\theta)$ and k_{02} an asymmetry between the upper and lower frequencies. k_{31} gives an asymmetry between $\theta > 0$ and $\theta < 0$, which is allowed by the lack of mirror symmetry in the crystal structure. The Fermi surface that results from summing these components is shown at right.

straddles E_F is clearly visible (Fig. 9 of Ref. [13]), and remains apparent in full $PdCoO_2$ band structures.

To analyze our data and compare with previous calculation, we performed electronic structure calculations on $PdCoO_2$ using the general potential linearized augmented plane wave method as implemented in the WIEN2K package [26]. We calculated 20 000 k points in the full Brillouin zone, and studied the effects of an on-site repulsion U_{eff} at the Co atoms. For $U_{\text{eff}} = 0$, we recover previously reported results, and find dHvA masses of around $1.9m_e$, larger than the measured value. Introducing a modest U_{eff} reduces the calculated masses toward the experimental values and simultaneously gives a ratio between k_{31} and k_{01} that is in better agreement with experiment (Table I). The high sensitivity of the in-plane masses, which arise from Pd-Pd bonding, to the Co site Coulomb repulsion appears surprising. A possible interpretation is that the Pd $5s$ component is extended enough to be sensitive to the charge distribution in the CoO_2 layers; this should be the subject of further investigation.

Although conduction by $5s$ states might account for the scale of the conductivity of $PdCoO_2$ at room temperature,

TABLE I. LDA + U results, and experimental data. U_{eff} is the effective on-site Coulomb repulsion at the Co sites. m^*_Γ is the dHvA mass for the orbit in the $k_z = 0$ plane, and m^*_Z the $k_z = \pm\pi$ plane.

	m^*_Γ	m^*_Z	k_{01} (Å^{-1})	k_{31} (Å^{-1})	k_{31}/k_{01}
$U_{\text{eff}} = 0$ eV	$1.90m_e$	$1.82m_e$	0.0039	0.0172	4.4
$U_{\text{eff}} = 5$ eV	1.66	1.52	0.0181	0.0029	0.2
Experiment	1.53	1.45	0.0107(3)	0.0010(3)	0.1

the low temperature resistivity has additional intriguing features. Measurement is challenging because of the tiny resistance of typical samples. By using transformers mounted at 1 K to provide low-noise (150 pV/$\sqrt{\text{Hz}}$) passive amplification, we obtained the data shown in Fig. 3. The difference between ρ_c and ρ_{ab} is striking: while ρ_c shows a T^2 dependence at low temperatures, ρ_{ab} becomes almost temperature-independent.

Below 30 K, $\rho_{ab}(T)$ is much better described by an activated form than the usual electron-phonon T^5 form (Fig. 3). This may be a consequence of phonon drag, in which the phonon population is pushed out of equilibrium by charge carrier flow. It is a well-known phenomenon in low-temperature thermopower, but has been seen in resistivity only in the alkali metals [27]. In clean materials momentum is transferred to the lattice through umklapp processes. For the alkali metals and for in-plane conduction in $PdCoO_2$, the Fermi surface is closed, resulting in an activation energy $k_B T_U = \hbar c k_U$, where k_U is the minimum wave number for umklapp processes (illustrated in Fig. 3) and c is the speed of sound. For $T \ll T_U$, electron-phonon scattering transfers momentum between electrons and phonons but does not relax the momentum of the combined system. $k_U \approx 0.5$ Å^{-1} in $PdCoO_2$. Fits to $\rho_{ab}(T)$ for two samples yield activation temperatures of 165 (Fig. 3) and 168 K (not shown), giving $c \approx 4400$ m/s. This is in fair agreement with specific heat measurements, where the magnitude of the T^3 term, 0.0619 mJ/mol K^4 [9], yields, for isotropic sound propagation, $c = 3650$ m/s. This analysis works equally well for potassium [28].

Fermi liquids usually have a T^2 low-temperature resistivity due to electron-electron scattering. A_c in

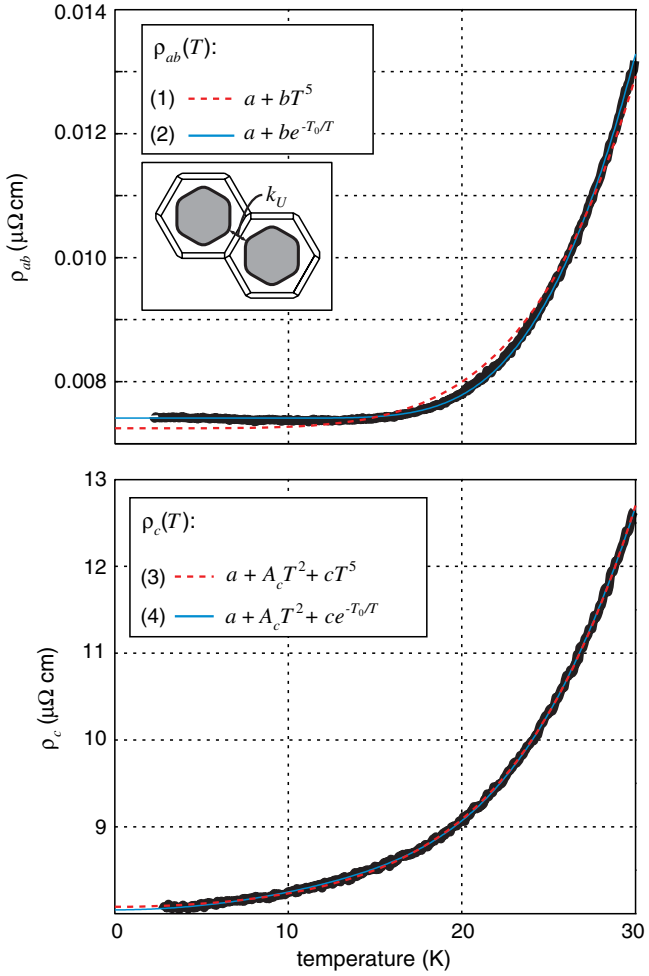

FIG. 3 (color online). In-plane $PdCoO_2$ resistivity $\rho_{ab}(T)$ (top), and c-axis resistivity $\rho_c(T)$ (bottom), with fits. At low T, ρ_c has a T^2 dependence, while ρ_{ab} is nearly temperature-independent. The inset in the top panel illustrates k_U, the minimum wave number for umklapp scattering. Partial fit results: (2) $T_0 = 165$ K. (3) $A_c = 1.4 \times 10^{-9}$ $\Omega\,\mathrm{cm/K^2}$. (4) $A_c = 2.1 \times 10^{-9}$ $\Omega\,\mathrm{cm/K^2}$, $T_0 = 157$ K.

$\rho_c(T) = \rho_c(0) + A_c T^2$ is 2×10^{-9} $\Omega\,\mathrm{cm/K^2}$. $\rho_{ab}(T)$ shows a very small resistivity upturn at low T, and the upper limit we can place on A_{ab} is 1.0×10^{-12} $\Omega\,\mathrm{cm/K^2}$. This is not a particularly small value for metals with electronic specific heats comparable to $PdCoO_2$ [31], but it is significantly smaller than A_c scaled by the low-T resistive anisotropy ($\rho_c(0)/\rho_{ab}(0) = 1000$). In the alkali metals K and Na the closed FS geometry is known to partially suppress electron-electron umklapp processes, reducing A by about a factor of 10 [32]. Such a suppression is also likely to apply to A_{ab} of $PdCoO_2$.

The combination of resistivity and dHvA data also shows that transport electron-phonon coupling in $PdCoO_2$ is very small over an extended temperature range. In Ref. [9], $\rho_{ab}(T)$ of $PdCoO_2$ for $0 < T < 500$ K is fitted to a sum of the Bloch-Gruneisen form and an Einstein mode contribution. These fits return Debye and Einstein temperatures Θ_D and Θ_E, and transport electron-phonon couplings scaled by the the plasma frequency squared, $\lambda_{D,\mathrm{tr}}/\Omega_p^2$ and $\lambda_{E,\mathrm{tr}}/\Omega_p^2$ [33]. The dHvA data here allow determination of the plasma frequency: $\Omega_{p,xx}^2 = ne^2/m\epsilon_0 = (7.2(1) \times 10^{15}\ \mathrm{sec}^{-1})^2$. Performing the same fit over the range $60 < T < 300$ K, where the lower bound excludes the region strongly affected by phonon drag, we obtain $\Theta_D = 329$ K and $\Theta_E = 1106$ K, in good agreement with [9]. $\lambda_{D,\mathrm{tr}}$ and $\lambda_{E,\mathrm{tr}}$ come to 0.043 and 0.023, respectively, which are exceptionally low values: Cu has $\lambda_{D,\mathrm{tr}} = 0.13$ and Ca, a metal with a particularly low dHvA mass of $\sim 0.6 m_e$, 0.05 [34]. These low couplings may also be due to the FS topology, through a partial suppression of umklapp processes at temperatures $T \sim T_U$. Careful calculation would be required to test this hypothesis.

Our measured residual resistivities $\rho_{ab}(T \to 0)$, between 0.007 and 0.008 $\mu\Omega$ cm for two samples, are very low, corresponding to a transport mean free path of 20 μm, or, in a standard interpretation, a defect density in the Pd layers of one in 10^5 [35]. This is a remarkable value for flux-grown crystals. To set it in context, the fractional quantum Hall effect has recently been observed in ZnO-based heterostructures, where, after years of research, the transport mean free path has been increased to ~ 1.5 μm [36]. This is considerably less than what we report here for a naturally two-dimensional material, motivating the study of delafossites as a natural material for multilayer oxide technologies.

In summary, we have observed exceptionally high conductivity in $PdCoO_2$ and mapped its Fermi surface in detail using the de Haas–van Alphen effect. Our data suggest that the conductivity of $PdCoO_2$ is due primarily to Pd $5s$ overlap. For in-plane transport, the contributions to resistivity from electron-phonon, electron-electron and electron-impurity scattering are all anomalously low. The effect of the closed Fermi surface topology on umklapp processes seems to play a role and is worthy of investigation. It is also possible, however, that scattering is suppressed by some non-standard mechanism not considered in the analysis we have presented. Our results provide motivation for further work on this fascinating material.

We acknowledge useful discussions with J. W. Allen, C. Varma, C. A. Hooley, D. J. Singh, and S. Yonezawa and practical assistance from P. A. Evans. This work has made use of the resources provided by the Edinburgh Compute and Data Facility (ECDF), which is partially supported by the eDIKT initiative. We acknowledge funding from the UK EPSRC, the MEXT KAKENHI (No. 21340100), the Royal Society, and the Wolfson Foundation.

*apm9@st-andrews.ac.uk

[1] M. A. Marquardt, N. A. Ashmore, and D. P. Cann, Thin Solid Films **496**, 146 (2006).

[2] R. D. Shannon, D. B. Rogers, and C. T. Prewitt, Inorg. Chem. **10**, 713 (1971); C. T. Prewitt, R. D. Shannon, and D. B. Rogers, Inorg. Chem. **10**, 719 (1971).

[3] D. B. Rogers, R. D. Shannon, C. T. Prewitt, and J. L. Gillson, Inorg. Chem. **10**, 723 (1971).

[4] H. Yanagi, T. Hase, S. Ibuki, K. Ueda, and H. Hosono, Appl. Phys. Lett. **78**, 1583 (2001), and references therein.

[5] H. Takatsu, S. Yonezawa, S. Fujimoto, and Y. Maeno, Phys. Rev. Lett. **105**, 137201 (2010).

[6] D. J. Singh, Phys. Rev. B **76**, 085110 (2007).

[7] F. Wang and A. Vishwanath, Phys. Rev. Lett. **100**, 077201 (2008).

[8] P. F. Carcia, R. D. Shannon, P. E. Bierstedt, and R. B. Flippen, J. Electrochem. Soc. **127**, 1974 (1980).

[9] H. Takatsu, S. Yonezawa, S. Mouri, S. Nakatsuji, K. Tanaka, and Y. Maeno, J. Phys. Soc. Jpn. **76**, 104701 (2007).

[10] H.-J. Noh, J. Jeong, J. Jeong, E.-J. Cho, S. B. Kim, Kyoo Kim, B. I. Min, and H.-D. Kim, Phys. Rev. Lett. **102**, 256404 (2009).

[11] M. Tanaka, M. Hasegawa, and H. Takei, J. Phys. Soc. Jpn. **65**, 3973 (1996).

[12] V. Eyert, R. Frésard, and A. Maignan, Chem. Mater. **20**, 2370 (2008).

[13] R. Seshadri, C. Felser, K. Thieme, and W. Tremel, Chem. Mater. **10**, 2189 (1998).

[14] Kyoo Kim, H. C. Choi, and B. I. Min, Phys. Rev. B **80**, 035116 (2009).

[15] K. P. Ong, Jia Zhang, J. S. Tse, and Ping Wu, Phys. Rev. B **81**, 115120 (2010).

[16] I. Nagai, N. Shirakawa, S.-I. Ikeda, R. Iwasaki, H. Nishimura and M. Kosaka, Appl. Phys. Lett. **87**, 024105 (2005).

[17] T. P. Pearsall and C. A. Lee, Phys. Rev. B **10**, 2190 (1974).

[18] J. R. Cooper, A. Carrington, P. J. Meeson, E. A. Yelland, N. E. Hussey, L. Balicas, S. Tajima, S. Lee, S. M. Kazakov, and J. Karpinski, Physica C (Amsterdam) **385**, 75 (2003).

[19] D. Shoenberg, *Magnetic Oscillations in Metals* (Cambridge University Press, Cambridge, England, 1983).

[20] C. Bergemann, A. P. Mackenzie, S. R. Julian, D. Forsythe, and E. Ohmichi, Adv. Phys. **52**, 639 (2003).

[21] P. D. Grigoriev, Phys. Rev. B **81**, 205122 (2010).

[22] See Supplemental Material at http://link.aps.org/supplemental/10.1103/PhysRevLett.109.116401 for discussion of the harmonic analysis of the FS, mass determination, resistive anisotropy, a tight-binding calculation, and Dingle analysis.

[23] F. M. Mueller, A. J. Freeman, J. O. Dimmock, and A. M. Furdyna, Phys. Rev. B **1**, 4617 (1970).

[24] D. H. Dye, S. A. Campbell, G. W. Crabtree, J. B. Ketterson, N. B. Sandesara, and J. J. Vuillemin, Phys. Rev. B **23**, 462 (1981).

[25] M. Tanaka, M. Hasegawa, T. Higuchi, T. Tsukamoto, Y. Tezuka, Shik Shin, and H. Takei, Physica B (Amsterdam) **245**, 157 (1998).

[26] P. Blaha, K. Schwarz, G. K. H. Madsen, D. Kvasnicka, and J. Luitz, computer code WIEN2K, Technische Universität Wien, Austria, 2001.

[27] J. Bass, W. P. Pratt, and P. A. Schroeder, Rev. Mod. Phys. **62**, 645 (1990).

[28] The T^3 term of the specific heat of potassium is 2.57 $\mathrm{mJ/mol\,K^4}$ [29], yielding $c = 1290$ m/s. $k_U = 0.24$ $\mathrm{\AA^{-1}}$, so $\hbar c k_U/k_B = 24$ K, in good agreement with the activation temperature obtained from fitting $\rho(T)$: 23 K [30].

[29] W. H. Lien and N. E. Phillips, Phys. Rev. **133**, A1370 (1964).

[30] D. Gugan, Proc. R. Soc. A **325**, 223 (1971).

[31] Aluminum, for example, has $\gamma = 1.35$ $\mathrm{mJ/mol\,K^2}$ [E. H. Buyco and F. E. Davis, J. Chem. Eng. Data **15**, 518 (1970)], similar to $PdCoO_2$, and $A = 2.8 \times 10^{-13}$ $\Omega\,\mathrm{cm/K^2}$ [32].

[32] M. Kaveh and N. Wiser, Adv. Phys. **33**, 257 (1984).

[33] P. B. Allen and W. W. Schulz, Phys. Rev. B **47**, 14434 (1993).

[34] P. B. Allen, Phys. Rev. B **36**, 2920 (1987).

[35] A standard Dingle analysis of the dHvA oscillations yields a much lower mean free path of 0.6 μm [22]. However this result should be treated with caution, because as conductivity becomes very high phase smearing due to internal field inhomogeneity becomes more problematic. Observing a Dingle mean free path matching the transport mean free path of 20 μm would require a field homogeneity of one in 10^5, probably difficult to achieve in a material with known Co-based, magnetic impurity phases [9].

[36] A. Tsukazaki, S. Akasaka, K. Nakahara, Y. Ohno, H. Ohno, D. Maryenko, A. Ohtomo, and M. Kawasaki, Nature Mater. **9**, 889 (2010).